Chemical Engineering Journal 545 (2026) 179611

Contents lists available at ScienceDirect

Chemical Engineering Journal

journal homepage: www.elsevier.com/locate/cej

Enzymatic reaction kinetics within Pickering emulsions through progress-curve analysis

Maximilian Seiler [a,*], Thomas Waluga [b], Anja Drews [a]

[a] Process Engineering in Life Science Engineering, HTW Berlin, Wilhelminenhofstraße 75 A, 12459 Berlin, Germany
[b] Institute of Process Systems Engineering, Hamburg University of Technology, Am Schwarzenberg-Campus 4, 21073 Hamburg, Germany

ARTICLE INFO

Dataset link: Experimental Data and code (Original data)

Keywords:
Pickering emulsion
Enzyme kinetics
Biocatalysis
Progress curve
Biphasic

ABSTRACT

Pickering emulsions are attracting increasing attention in biphasic biocatalysis because their particle-stabilized interfaces provide a large contact area between enzymes in the aqueous phase and water-insoluble substrates. Despite growing interest, a comprehensive kinetic framework for enzymatic reactions in Pickering emulsions remains lacking. Here, a progress-curve-based kinetic description of a hydrolysis reaction is presented for the first time and compared with both a single-phase system and a particle-free biphasic system.

Transitioning from an aqueous single-phase system to a biphasic system the maximum reaction velocity v_{max} increased threefold, while the apparent Michaelis–Menten constant increased by four orders of magnitude, indicating significant interfacial mass-transfer contributions. Notably, Michaelis–Menten kinetics derived from initial rates failed to predict product formation at elevated concentrations due to product inhibition.

Direct fitting of integrated rate equations to full progress curves enabled efficient parameter estimation and captured product inhibition while substantially reducing experimental effort compared to conventional initial-rate analysis. Both competitive and non-competitive inhibition models adequately described the data. Comparison with a particle-free biphasic system revealed similar kinetics at high stirring rates; however, under reduced energy input, the Pickering emulsion retained its kinetic parameters and activity, whereas the biphasic system became mass-transfer limited. Overall, this study establishes macrokinetic parameters for Pickering emulsions using progress-curve analysis and demonstrates their advantages under low-stirring conditions, providing a basis for process development.

1. Introduction

Pickering emulsions, first reported by Ramsden [1] and Pickering [2], are emulsions stabilized by solid particles at the interface. Due to a reduction in interfacial free energy, particles strongly adsorb at a liquid-liquid interface and act as a mechanical barrier for coalescence [3,4]. Over the past decades, Pickering emulsions have attracted increasing attention as platforms for biphasic biocatalysis [5]. The practically irreversible attachment of particles to the interface stabilizes droplets and provides a large interfacial area between the aqueous and organic phases. As a result, Pickering emulsions often exhibit enhanced catalytic efficiency compared to conventional biphasic systems, especially for hydrophobic substrates [6–10]. Beyond the increased interfacial area, the particle-covered interface may directly influence adsorption processes and catalytic activity at the interface [11]. Various enzymatic reactions have been carried out in Pickering emulsions, including esterification [6,10,12], transesterification [13–15], epoxidation [16–18], hydrolysis [19,20], and carboligation [21]. Reactions in Pickering emulsions are mostly performed in batch processes [17,22], but have also been investigated in continuous flow systems [16,18].

In order to optimize such processes and facilitate their scale-up towards industrial applications, a descriptive model of the reaction kinetics within Pickering emulsions is required. The existing literature on biocatalysis in Pickering emulsions mainly focuses on assessing and preserving the enzymatic activity, whereas comprehensive kinetics are mostly lacking. Although some studies reported kinetic parameters by fitting Michaelis–Menten parameters (K_M and v_{max}) based on initial rate experiments as secondary outcomes [18,23], a systematic framework is still missing. Therefore, the aim of this study is to provide an approach for estimating the parameters of a reaction rate law of an enzymatic catalysis in a Pickering emulsion.

The most fundamental description of enzymatic reactions is the Michaelis–Menten concept (Eq. (3)) [24]. Although originally developed to describe homogeneous enzyme catalysis, it has also been applied as a basis for modeling interfacial enzyme kinetics [25–27]. More

* Corresponding author.
E-mail address: maximilian.seiler@htw-berlin.de (M. Seiler).

https://doi.org/10.1016/j.cej.2026.179611
Received 25 March 2026; Received in revised form 10 June 2026; Accepted 16 July 2026
Available online 22 July 2026

broadly, even concepts from heterogenous (non-biochemical) catalysis (e.g. Sabatier principle) have likewise been adopted for interfacial biocatalysis to further analyze interfacial biocatalytic processes [28–30]. Although these concepts are mechanistically profound, detailed knowledge of substrate and product mass transfer, adsorption phenomena and enzyme coverage of the interface is needed. Additionally, determining the exact location of the active center within the interfacial region remains a significant challenge [11]. Consequently, this may result in necessary assumptions and simplifications. While Rusli et al. were able to model the hydrolysis of sunflower oil with *Candida rugosa* lipase using reversible Michaelis–Menten kinetics in a biphasic system with high accuracy [31], they had to assume enzyme monolayers and disregarded potential inhibition. However, previous studies demonstrated that lipases adsorb in multilayers within Pickering emulsion droplets [32].

A more practical approach is to describe the reaction rate using a macrokinetic model, in which mass transfer, adsorption, and interfacial phenomena are incorporated into apparent kinetic parameters. In this case, both substrates as well as products are quantified in the organic phase, although the reaction may occur at the interface or within the aqueous phase. The most common descriptor of a reaction rate is the enzymatic activity U, defined as is the amount of product formed per minute and volume in μmol L^{-1} min^{-1}. It is typically determined from the initial rate of product formation or substrate depletion [33]. While this approach offers the advantage of being largely insensitive to enzyme deactivation or product inhibition during the early stages of the reaction, the parameters obtained in this manner may exhibit significant variability and may not adequately represent the overall reaction progress. For one, there is no unified consensus on how the initial rate should be defined [34]. Second, assessing the extent of product inhibition can be technically challenging when analytical accuracy is limited and requires additional experimental effort.

Alternatively, product or substrate concentration can be measured beyond the initial rate regime and followed until reaction completion to obtain a full-progress curve. An integrated form of the rate equation is then applied in analytical or numerical procedures to determine the optimal kinetic parameters. Although progress-curve analysis was already used in the original work by Michaelis and Menten [24], it remains rather scarcely employed in the field of biocatalysis. Numerous studies have highlighted its advantages, including improved parameter accuracy and reduced experimental effort [33–38].

For batch-processes, the integrated Michaelis–Menten equation in its explicit form (Eq. (4)) is used to determine the kinetic parameters. This closed-form solution was first derived by Beal [39], but initially received little attention [40]. An explicit analytical solution, based on the quasi-steady-state-approximation (QSSA), was later presented by Schnell and Mendoza using the Lambert-W function [41]. Subsequently, closed-form solutions of the Michaelis–Menten equation were expanded to account for competitive, uncompetitive and non-competitive inhibitors [33,42,43]. Even competitive product inhibition can be described explicitly with the Lambert-W function [40].

In this study, the kinetics of a lipase-catalyzed hydrolysis reaction were investigated in a water-in-oil (W/O) Pickering emulsion. In the first part (Section 3.1), Michaelis–Menten parameters obtained from initial-rate experiments are compared for an aqueous system and a Pickering emulsion. The effect of product inhibition is demonstrated and then further analyzed using different inhibition models in a progress-curve analysis (Section 3.2).

In Section 3.3, the kinetic parameters are further compared with those of a particle-free biphasic system. Finally, in Section 3.4, the same comparison is performed under reduced stirring conditions to deliberately induce mass-transfer limitations.

2. Materials and methods

2.1. Chemicals

Lipase Type VII from *Candida rugosa* (CRL) was purchased from Sigma Aldrich (Merck KGaA, Darmstadt, Germany). Di-sodium hydrogen phosphate dihydrate and sodium di-hydrogen phosphate dihydrate were purchased from Carl Roth GmbH + Co.KG (Karlsruhe, Germany). 1-octanol (99%) was purchased from Th.Geyer (Renningen, Germany). Dimethyloctadecyl[3-(trimethoxysilyl)propyl]ammonium chloride (60%) was obtained from Acros Organics (Geel, Belgium). p-Nitrophenylbutyrate (95%) was obtained from BLDpharm (Shanghai, China) and p-Nitrophenole was obtained from Alfa Aesar (Haverhill, USA). Absolute ethanol (99.9%) was obtained from VWR chemicals BDH (Darmstadt, Germany).

2.2. Synthesis of surface modified silica particles

A detailed description of the procedure can be found in [44,45]. In short, Ludox TM-40 particles (Sigma-Aldrich) were dialyzed and a suspension of about 1 wt% in ethanol was prepared. For the positively charged surface modification, dimethyloctadecyl[3-(trimethoxysilyl) propyl]ammonium chloride was used. The positive charge is located at the quaternary amine and therefore not pH dependent. Afterwards, the solvent was completely removed using a rotary evaporator. The obtained particles were washed multiple times with Milli-Q water and once with a 30 vol% ethanol solution. The particles were obtained as a dry powder and are approximately 30 nm in size and partially hydrophobic (air–water contact angle: 105–110°). The positively charged particles contain a charge of 53 mV in ethanol.

2.3. Preparation of W/O Pickering emulsions

For the preparation of the Pickering emulsions, nanoparticles were dispersed in dry 1-octanol using an ultrasonicator for 30 min at a weight fraction of 0.5 wt% relative to the total mass. Lyophilized lipase was dissolved in an aqueous phosphate buffer at a concentration of 1 g L^{-1} with respect to the aqueous phase. The two phases were then mixed using an IKA T 25 digital UltraTurrax S25N-18G at 17 600 min^{-1} for 2 min. The volumetric fraction of the aqueous phase was maintained at $\phi = 0.2$ after substrate addition.

2.4. Reaction

The reaction investigated is the hydrolysis of p-nitrophenyl butyrate (p-NPB) to p-nitrophenol (p-NP) and butyric acid (Fig. 1), which is one of the most commonly used model reactions for measuring lipase activity [46–50]. While the pure substrate p-NPB is not detectable in the aqueous phase and is therefore practically insoluble in water, the product p-NP is slightly soluble in the aqueous phase. 1-octanol was chosen as the continuous phase due to its unlimited solubility for p-NPB, high solubility for p-NP (>1.5M), and the formation of Pickering emulsions that remained stable for several weeks. The partition coefficient $P = c_{P,oil}/c_{P,aq}$ of p-NP between 1-octanol and phosphate buffer (100 mM, pH 7) was determined to be at 31.17 (see Figure S1).

The product concentration was measured in the oil phase and corrected using Eq. (1) to account for the amount of product that partitioned into the aqueous phase,

$$c_P = c_{P,oil} \cdot \left(1 + \frac{1}{P} \cdot \frac{\phi}{1-\phi}\right) \quad (1)$$

where c_P is the total concentration of the product p-NP, ϕ the aqueous phase fraction and P the partition coefficient. A detailed derivation of Eq. (1) is provided in the supplementary material. Because measurements at $t = 0$ are unreliable, the initial substrate concentration was

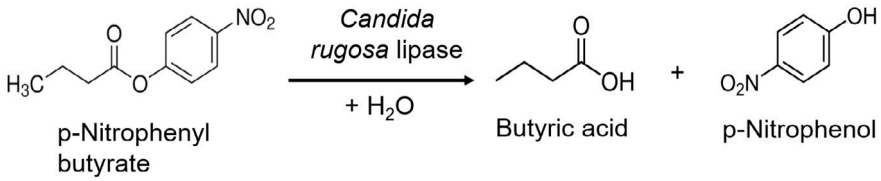

Fig. 1. Reaction scheme of the enzymatic hydrolysis of p-Nitrophenylbutyrate.

calculated as the average of the sum of product and substrate over all data points i, assuming a selectivity of 1:

$$c_{S_0} = \frac{\sum_i (c_{P,i} + c_{S,i})}{i} \tag{2}$$

Since the total amount of substrate and product was found to remain constant over the course of the reaction, side reactions can be considered negligible, and the assumption of a selectivity of 1 is therefore justified. Only at high product concentrations, clouding of the organic phase was observed, particularly noticeable in the absence of particles, where phase separation occurred in the samples. This product crystallization manifested as a reduced rate of increase in product concentration at higher concentrations. Product precipitation did not affect the reaction rate, as the substrate concentration continued to decline at the expected rate. For the overall kinetic fitting, data points above 1.2 M product were therefore fitted using $c_P = c_{S_0} - c_S$ for the product concentration.

2.5. Measurement setup

Batch reactions were carried out in a stirred cell (XFUF04701, Merck KGaA, Darmstadt, Germany), which is commonly used in continuous membrane processes [13,16]. This setup offers the advantage that the magnetic stir bar is positioned 3–4 mm above the bottom of the cell. This prevents the descruction of droplets due to shearing at the bottom. Usually, 10 mL of the prepared Pickering emulsion were placed inside the stirred cell. The total volume differed slightly between experiments to avoid wasting substrate at higher concentrations, but the stir bar was always fully submerged. Temperature was controlled at 30 °C via a water bath connected to a thermostat. The magnetic stirrer was kept at either 100 or 300 min^{-1}. With a stirrer diameter of 2.5 cm this relates to a stirrer tip speed of 0.18 m/s and 0.55 m/s. The reaction was initiated by the addition of the substrate. Samples were withdrawn over the course of the reaction and immediately transferred into reaction vessels containing 1 mL of ice-cooled phosphoric acid (2 M) to quench the reaction (see Figure S5). The samples were then briefly centrifuged (0.5 min, 15 000 min^{-1}), and the upper phase was collected and diluted with acetonitrile prior to HPLC analysis.

For initial rate measurements, the same experimental setup was used, but samples were only taken within the first 15 min. Usually, four points were used to fit a linear function, the slope of which was taken as the reaction rate r in mM/min. All points were below a conversion of 10%.

2.6. Single phase kinetics

The method for determining kinetic parameters in the aqueous phase was adopted from Rúa et al. [50]. Briefly, 1 mL of a 0.01 g L^{-1} CRL solution in phosphate buffer (100 mM, pH 7) was prepared, and p-NPB was dissolved in acetone at concentrations between 0.56 and 28 mM. The reaction was initiated by adding 41.8 µL of the prepared p-NPB solution to the enzyme mixture, resulting in a final acetone content of 4 %. The formation of p-NP was monitored spectrophotometrically at a wavelength of 346 nm using a UV–Vis spectrometer (UV-1900, Shimadzu, Kyoto, Japan).

2.7. Protein content

The actual enzyme amount was approximated through the total protein amount measured by the Bradford method [51]. A BSA-solution (98% purity) was used as the calibration standard. 1 g/L crude CRL solution was dissolved in phosphate buffer (pH7, 100 mM) and the absorption was measured at 595 nm with a TECAN infinite M200 plate reader after the addition of the Bradford reagent.

2.8. Kinetic modeling and parameter estimation

Regarding a single substrate reaction without any type of inhibition, the Michaelis–Menten equation describes the reaction rate as a function of the substrate:

$$r = -\frac{dc_S}{dt} = \frac{v_{\max} \cdot c_S}{K_M + c_S} \tag{3}$$

Under quasi-steady-state conditions for the enzyme–substrate complex, K_M is the Michealis-Menten constant, v_{max} is the limiting reaction velocity under substrate saturation, and k_{cat} is the dissociation constant towards the product. The solution of Eq. (3) may be analytically derived using the Lambert-W function and provides a description of the product formation in correlation of the initial substrate concentration c_{S_0} and t: [39,41]:

$$c_P(t) = c_{S_0} - c_S(t) = c_{S_0} - K_M \cdot W\left(\frac{c_{S_0}}{K_M} exp\left(\frac{-v_{max}t + c_{S_0}}{K_M}\right)\right) \tag{4}$$

For hydrolysis reactions, strictly speaking, Eq. (4) is not fully sufficient, as a ping–pong bi–bi or sequential mechanism should be considered. However, since water is present in large excess, the hydrolysis kinetic is assumed to be a pseudo uni–bi reaction. In biphasic reaction systems, this assumption must be examined carefully. At the highest substrate concentration used in this study, the molar excess of water decreases to a minimum value of 7.74.

Molecules that block the active site of an enzyme, so-called inhibitors, can reduce the apparent reaction rate. For reversible binding at the active site, inhibition is commonly classified as competitive, uncompetitive, or non-competitive. In the case of product inhibition, the inhibitor is the reaction product itself. When the product is able to bind competitively to the free enzyme, the reaction would in principle be reversible if water was not present in large excess. However, due to the high water concentration, the equilibrium is strongly shifted towards the product side, resulting in apparent product inhibition rather than a measurable reverse reaction. Experiments conducted with p-NP and butyric acid at initial concentrations above 1 M support this assumption, as no formation of p-NPB or decline in p-NP concentration was observed. For competitive product inhibition, where the product competes with the substrate for binding to the free enzyme, the Michaelis–Menten equation (Eq. (4)) can be extended as follows:

$$r = -\frac{dc_S}{dt} = \frac{v_{\max} \cdot c_S}{K_m\left(1 + \frac{c_P}{K_P}\right) + c_S} \tag{5}$$

where K_P is the inhibition constant of p-NP. Since butyric acid did not significantly influence the reaction, its inhibition constant was

neglected. For competitive product inhibition the rate equation (5) can be solved analytically [38,40]:

$$c_P(t) = c_{S_0} - K_M^* \cdot W\left(\frac{c_{S_0}}{K_M^*} exp\left(\frac{-v_{max}^* t + c_{S_0}}{K_M^*}\right)\right) \tag{6a}$$

$$v_{max}^* = \frac{v_{max}/K_M}{1/K_M - 1/K_P} \tag{6b}$$

$$K_M^* = \frac{1 + c_{S_0}/K_P}{1/K_M - 1/K_P} \tag{6c}$$

In this study, the kinetic parameters (K_M, K_P and v_{max}) were estimated by minimizing the weighted residuals between the experimentally measured product concentration over the full progress curve and the corresponding model prediction using the *least_squares* function in Python. To prevent overfitting at higher product concentrations, residuals were weighted by the standard deviation σ, which was obtained from an estimate of the measurement uncertainty for each data point. This includes uncertainty from calibration and pipetting. For further details see Supplementary equations 5-7. To ensure robust identification of the global optimum, multiple initial parameter guesses were generated using a Hammersley sequence to uniformly sample the parameter space. Each initialization was solved independently, and the parameter set yielding the lowest sum of squared residuals (SSR) was selected as the optimal solution.

Non-competitive and uncompetitive product inhibition were integrated from the respective rate laws (Eqs. (7) and (8)), but cannot be expressed in closed analytical form. Therefore, the resulting implicit function (see Supplementary equation 8 and 9) was solved with a root-finding algorithm, $f(S,t) = 0$, using the *root_scalar* function for each data point, and the parameters were fitted analogously using *least_squares*.

$$r = -\frac{dc_S}{dt} = \frac{v_{\max} c_S}{(K_m + c_S)\left(1 + \frac{c_P}{K_P}\right)} \tag{7}$$

$$r = -\frac{dc_S}{dt} = \frac{v_{\max} c_S}{K_m + c_S\left(1 + \frac{c_P}{K_P}\right)} \tag{8}$$

To assess the quality and precision of parameter estimates, confidence intervals for each parameter were calculated. The parameter covariance matrix was approximated by linearizing the nonlinear least-squares problem around the optimum using a first-order Taylor expansion [52]. Under this local linear approximation, the covariance matrix of the parameter estimates $\hat{\Theta}$ is given by

$$Cov(\hat{\Theta}) = \hat{\sigma}^2 \cdot (J^T J)^{-1} \tag{9}$$

where J is the Jacobian matrix. The residual variance $\hat{\sigma}^2$ was estimated as

$$\hat{\sigma}^2 = \frac{\sum_i (y_i - \hat{y}_i)^2}{n - k} \tag{10}$$

with n denoting the number of datapoints and k the number of fitted parameters. Assuming normally distributed residuals, the 95% confidence interval CI_{95} for each parameter was constructed using Student's t-distribution to account for the uncertainty in the estimated variance:

$$CI_{95} = t_{975,n-k} \cdot \sqrt{Cov(\hat{\Theta}_{j,j})} \tag{11}$$

2.9. Model evaluation

To evaluate and better compare different models with each other, multiple criteria were employed. The reduced chi-squared statistic χ_v^2 is commonly used to assess the goodness of fit:

$$\chi_v^2 = \frac{\sum_i \frac{(y_i - \hat{y}_i)^2}{\sigma_i^2}}{n - k} \tag{12}$$

χ_v^2 describes if the residuals are adequately explained by the estimated uncertainty σ_i. A $\chi_v^2 \gg 1$ correlates to a lack of fit or underestimated uncertainty, while a $\chi_v^2 \ll 1$ corresponds to overfitting or overestimated error.

Additionally, Akaike information criterion (AIC) and Bayesian information criterion (BIC) are calculated under a normal regression model according to:

$$AIC = 2k + n\ln\left(\frac{SSR}{n}\right) \tag{13}$$

$$BIC = k\ln(n) + n\ln\left(\frac{SSR}{n}\right) \tag{14}$$

Both AIC and BIC penalize additional number of parameters and provide a good indicator for model selection between differently complex models. Models with lower AIC and BIC are preferred. To evaluate the models capacity to predict new data and to avoid overfitting and selection bias [53], a leave-one-out-cross-validation (LOOCV) is performed. Systematically one run is left as a test set, while the remaining runs are used as the training set. The residual error over all left out runs is collected in the Predicted Residual Sum-of-Squares (PRESS) statistic, which is used to calculate the predicted R_{pred}^2:

$$R_{pred}^2 = 1 - \frac{PRESS}{SST} \tag{15}$$

where SST is the total sum of squares. Here, a R_{pred}^2 close to 1 corresponds to a good predictive capacity.

2.10. HPLC analysis

Samples were diluted in acetonitrile and measured with the Varian ProStar HPLC system (Varian, Inc., USA) equipped with Varian ProStar 335 photodiode array detector, Varian 460-LC autosampler and OTU Trikala C18,105 Å, 5μ, 150 × 3.0 mm column (Applichrom GmbH, Germany). An isocratic system (65 vol% acetonitrile, VWR GmbH, Germany and 35 vol% water) at constant flowrate of 1 mL min^{-1} was used. Injection volume was 10 µL and detector wavelength was set to 380 nm for higher concentrations and 300 nm for lower substrate concentrations. In this setup, p-NP had a rentention time of 1 min and p-NPB a retention time of 2.5 min.

3. Results and discussion

For a fair comparison between experiments, the influence of enzyme loading should be excluded by considering the specific reaction rate (activity) v, expressed in µmol min^{-1} mg^{-1}. In a single-phase system, this is readily achieved by dividing the reaction rate by the enzyme concentration, since both the enzyme and product are homogeneously distributed throughout the medium. In Pickering emulsions, however, the enzymes are confined to the aqueous phase [32], whereas the product is predominantly located in the organic phase. Therefore, the heterogeneous distribution of both species must be taken into account:

$$v = r \cdot \frac{V_{oil}}{V_{aq} \cdot c_E} = r \cdot \frac{(1-\phi)}{\phi} \cdot \frac{1}{c_E} \tag{16}$$

When referring to the maximum reaction rate v_{max} as a specific rate per mg enzyme, the notation u is used:

$$u = v_{max} \frac{(1-\phi)}{\phi} \cdot \frac{1}{c_E} \tag{17}$$

Since all Pickering emulsion experiments in this work were performed at a crude enzyme concentration of $c_E = 1$ g L_{aq}^{-1} and an aqueous phase fraction of $\phi = 0.2$, specific and non-specific reaction rates differ only by a constant factor of 4 L_{aq} g^{-1} and can therefore be used interchangeably. The droplet diameter was determined by microscopy to be approximately 10 µm (see Figure S9). To estimate the total amount of enzyme present, a Bradford assay was performed. Using the relative protein content of the unpurified enzyme preparation, the specific reaction rate can also be calculated based on the estimated enzyme

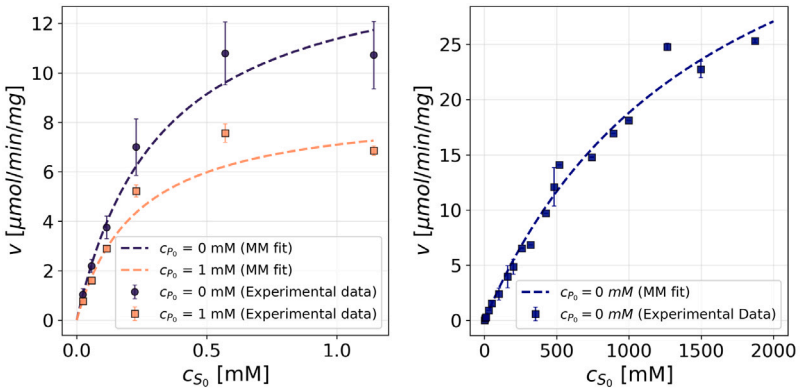

(a) Single-phase system (b) Pickering emulsion

Fig. 2. a: Specific reaction rate of CRL measured as initial reaction rate in: (a) a single-phase system with a CRL concentration of 0.01 g L^{-1} in phosphate buffer (pH7, 100 mM) with either 0 or 1 mM of p-NP present and (b) in a Pickering emulsion with 0.5 wt% particles and 1 g L^{-1} enzyme concentration. Error bars depict standard deviation of at least two measurements.

amount. Based on BSA calibration (Fig. S3), a protein content of 4.8 (± 0.17) wt%, corresponding to 0.048 g L^{-1}, was determined.

To assess potential enzyme deactiviation and Pickering emulsion stability, extended long-term experiments were performed. After 7 days of continuous shaking, lipase activity in both the Pickering emulsion and the biphasic system showed no significant reduction. After 40 days, however, the activity decreased to 76% of its initial value (see Figure S6). Based on these results, enzyme deactivation over the duration of the progress-curve measurements, which was up to 25 h, was considered negligible and was therefore not included in the kinetic analysis. To rule out enzyme deactivation by *p*-NP, initial-rate experiments were performed before and after exposure to *p*-NP. Following the removal of *p*-NP, the initial reaction rate remained unchanged, indicating no detectable loss of enzymatic activity (see Figure S7).

3.1. Comparison of kinetics in single-phase systems and Pickering emulsions

The experimental data of the reaction in the aqueous system as well as the Pickering emulsion along with the respective Michaelis–Menten fit are depicted in Fig. 2. The reaction rate is quantified by analyzing the slope of the intial rates at different initial substrate concentrations and described by the Michaelis–Menten equation (Eq. (3)). The kinetic parameters are presented in Table 1.

The single-phase system is substantially limited by the substrate and product solubility and additional co-solvents are needed. A further increase in substrate concentration beyond 1.2 mM resulted in the formation of a biphasic system. When the Pickering emulsion was used, the limiting reaction rate per enzyme increased roughly threefold, while the substrate concentration required for efficient catalysis rose drastically. This is reflected in the pronounced increase in K_M, which spans approximately four orders of magnitude, while $v_{\max}$ increased only by a factor of ~3. These comparatively high values for K_M are also observed in other studies concerning kinetics in biphasic media [31,54,55]. It is also possible that the solvent (1-octanol) inhibits the enzyme competitively, which results in an inflated K_M [55,56]. Such a loss in apparent affinity likely indicates mass transfer limitations, which are inherently captured in the kinetic measurements.

In a single-phase system, substrate affinity is governed primarily by enzyme–substrate association, catalytic turnover, and product dissociation.It should be noted, however, that due to the unique ability of lipases to adopt an "open" conformation upon adsorption at hydrophobic interfaces, they may form dimers with altered catalytic activity when such hydrophobic interfaces are absent [57]. In a biphasic system, however, the substrate must first diffuse to, and potentially through, the aqueous enzymatic layer. For Pickering emulsions of a similar composition and with a droplet diameter of approximately 5 µm, the thickness of this layer was previously determined to be approximately 0.75 µm [32]. Subsequently, the product must diffuse back into the oil phase. This additional diffusion resistance may effectively reduce the apparent association rate constant k_1, thereby inflating the observed value of K_M, which should therefore be regarded as an apparent K_M.

Table 1
Michaelis–Menten parameters obtained through initial rate measurements. v_{max} is based on the crude enzyme concentration of 1 g L^{-1} and k_{cat} on the estimated pure enzyme concentration of 0.048 g L^{-1} as determined by the Bradford assay (see Section 2.7).

	K_M [mM]	±	u [$\frac{\mu mol}{min\ mg}$]	±	k_{cat} [s^{-1}]	±
Single-phase (0 mM c_P)	0.32	0.19	15.1	5.7	297.9	112.5
Single-phase (1 mM c_P)	0.23	0.04	8.73	0.8	172.3	15.8
Pickering emulsion	1573	560	48.4	10.4	955.1	205.2

In addition, Hanson and Schnell demonstrated that kinetic parameters estimated using the Michaelis–Menten equation in regimes where the assumption $c_S \approx c_{S_0}$ during enzyme–substrate complex formation is not fulfilled can be overestimated by factors of 10–1000 [37,58]. This so-called reactant stationary assumption is unlikely to hold in the interfacial region in biphasic systems when substrate mass transfer is slower than enzyme–substrate complex buildup, further contributing to inflated apparent kinetic parameters. Nonetheless, the Pickering emulsion still surpasses the single-phase system by a great amount, if one considers the absolute amount of product that can be produced, without the solubility limitation of the aqueous system.

To investigate product inhibition, *p*-NP was added to the single-phase system initially. Comparing the curves in Fig. 2(a), as well as the corresponding fitted parameters, a statistically significant ($p < 0.05$) reduction in $v_{\max}$ was observed. Since the change in K_M was statistically insignificant, non-competitive product inhibition is the most likely mechanism.

To illustrate the applicability range of the kinetic model without product inhibition, the experimental data of the full-progress curves were compared to the Michaelis–Menten model (Eq. (4)) using the parameters obtained above. The resulting fit is shown in Fig. 3. The effect of product inhibition was already observed in the single-phase system (Fig. 2(a)), and therefore only limited predictive accuracy for the full reaction course in a Pickering emulsion can be expected.

As evident from the parity plot (Fig. 3(b)), the model describes the data reasonably well up to product concentrations of approximately 250–300 mM. Beyond this range, however, the model systematically overestimates the product concentration. From the Q-Q plot 3(c) it

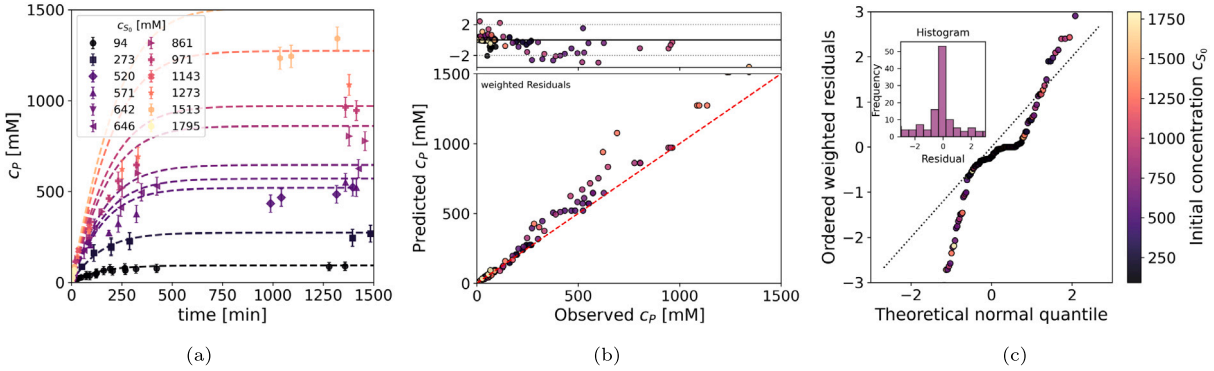

Fig. 3. (a) Product concentrations for the full reaction course are compared with the Michaelis–Menten model with parameters obtained by the initial rate analysis. Product concentration is calculated with Eq. (4). Error bars depict estimated error through analysis and pipetting. (b) Observed experimental data points vs. predicted product concentration, along with weighted residuals. (c) The Q-Q plot of the weighted residuals. Deviation from the identity line depicts deviation from a normal distribution.

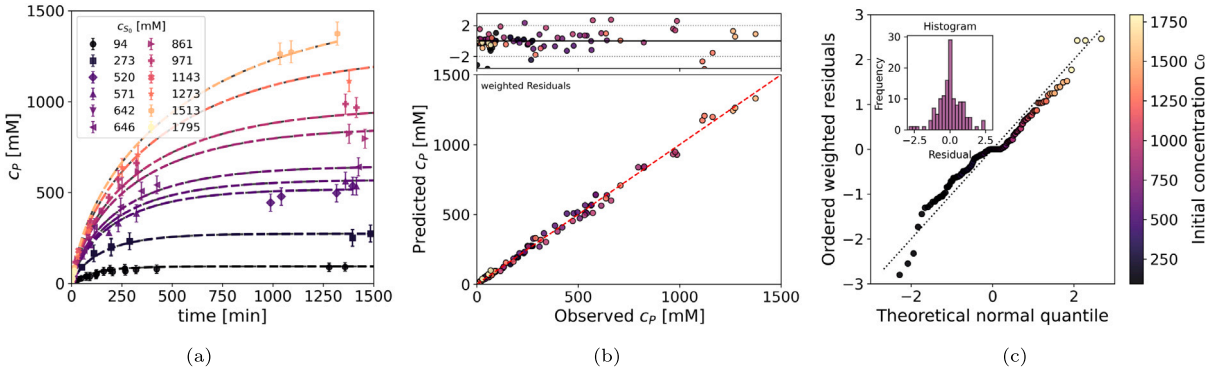

Fig. 4. (a) Non-competitive product inhibition (Eq. (7)) fitted onto full progress curve data. Error bars depict estimated error through analysis and pipetting. Measurements were taken in Pickering emulsions with 0.5 wt% particles and 1g/L enzymes. (b) Observed experimental data points vs. predicted product concentration, along with weighted residuals. (c) The Q-Q plot of the weighted residuals. Deviation from the identity line depicts deviation from a normal distribution.

is apparent, that these deviations are not normally distributed and originate from an insufficient model.

To accurately describe the full reaction course, a product inhibition term, c_P/K_P, must be included. Because determining product inhibition from initial-rate experiments is labor-intensive and experimental error may exceed analytical sensitivity in discontinuous sampling, progress-curve analysis was employed.

3.2. Product inhibition

The different inhibition models introduced in Section 2.8 are fitted onto the progress curve for the Pickering emulsion under non-limiting conditions and subsequently compared with each other. By way of example, Fig. 4 shows the results for the non-competitive enzyme inhibition. The fit of both competitive and uncompetitive are in the supplementary Figure S11.

The fitted parameters for all evaluated models, together with the corresponding model selection criteria, are summarized in Table 2. The non-competitive product inhibition model provides the best overall description of the experimental data. However, the reduced chi-squared value slightly below 1 suggests a minor degree of overfitting or an overestimation of the experimental uncertainty. Competitive product inhibition performs somewhat worse numerically, although the difference is small. This is not surprising, as both models involve similar inhibition mechanisms in which the product binds to the enzyme's active site. Notably, all parameter values obtained for the competitive inhibition model are estimated to be lower.

Uncompetitive product inhibition appears to fit the data reasonably well at first glance (Figure S11). However, closer inspection of the confidence intervals reveals that the estimated parameters are practically non-identifiable. The correlation matrix indicates strong parameter dependence, suggesting that the parameters cannot be solved independently. Uncompetitive inhibition implies that the product binds exclusively to the enzyme–substrate complex. Since the non-competitive model also incorporates this binding pathway, the uncompetitive formulation can partially reproduce the experimental behavior. However, because binding of the product to the free enzyme is not included, the model lacks sufficient constraints, resulting in poorly identifiable parameter estimates.

Since the product concentration is measured in the organic phase while the reaction occurs at the interface or within the aqueous phase, product mass transfer effects are implicitly incorporated into the estimated inhibition constant. The product inhibition constant, K_P, is therefore likely to be similarly inflated as K_M. This is indicated in Fig. 2(a) by the significant reduction in reaction rate at $c_P = 1$ mM in the single-phase system. As the reaction occurs at the interface, the local product concentration is elevated compared to the bulk phase. Consequently, the local inhibition constant at the interface is greater relative to the apparent inhibition constant in the bulk phase.

Despite its slightly reduced accuracy, the competitive inhibition model offers an important practical advantage to the non-competitive model: the product concentration can be expressed explicitly via the closed-form solution (Eq. (6a)), which substantially reduces computational effort. For 100 sets of initial parameter guesses, fitting the explicit competitive inhibition model required only 1.85 s. In contrast,

Table 2
Parameter estimates with the respective confidence intervals for different product inhibition alongside model evaluation criteria for Pickering emulsion stirred at 300 min^{-1}.

Inhibition type	u	CI[a] ±%	K_M	CI ±%	K_P	CI ±%	AIC	BIC	R^2_{adj}	χ^2_v	R^2_{pred}
None [prog. c.]	36.96	42.4	1525	61.4	–	–	1099	1105	0.963	3.347	0.960
None [init. r.]	48.40	21.5	1573	35.6	–	–	1171	1177	0.936	5.438	0.930
comp.	50.40	21.3	1196	31.5	151.5	18.4	845	854	0.994	0.848	0.993
uncomp.[b]	144.10	96.9	5375	107.0	32.9	102.4	920	929	0.991	1.365	0.983
noncomp.	60.68	20.6	1490	28.3	236.1	15.2	838	846	0.995	0.840	0.994

Notes: u in $\mu mol\,min^{-1}\,mg^{-1}$; K_M and K_P in mM.
[a] CI denotes the 95% confidence interval.
[b] Parameters are practically non-identifiable.

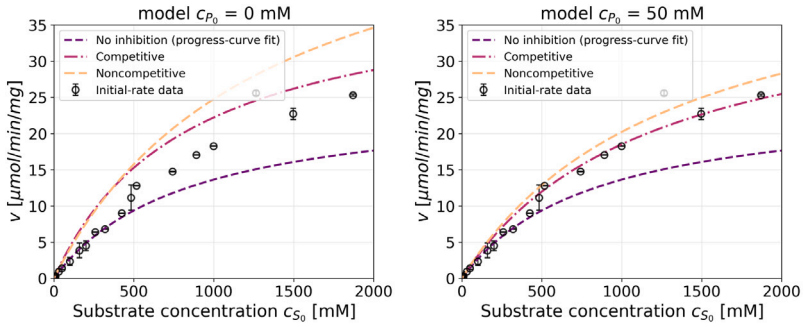

Fig. 5. Comparison of the models obtained by the progress curve analysis to the initial rate data both for (a) $c_{P,0}$ = 0 mM and (b) $c_{P,0}$ = 50 mM. Initial rates were taken within the first 15 min.

fitting the non-competitive model using numerical root finding required 321.5 s under identical conditions. For larger kinetic models, and particularly in cases where parameters are estimated dynamically, the competitive inhibition formulation may therefore represent the more efficient choice.

Additionally, the standard Michaelis–Menten model without inhibition was fitted for comparison. Similar to the initial rate analysis, this model describes the data reasonably well at lower product concentrations, where inhibition effects are less pronounced, but fails at higher concentrations (see Figure S11 g,h). Both the initial rate approach and the direct fit of the inhibition-free Michaelis–Menten model to the full progress curve yielded the poorest model selection criteria.

Since the Michaelis–Menten fit was compared to the progress-curve data, it is likewise appropriate to compare the inhibition models obtained from the progress-curve data to the initial rate measurements, as shown in Fig. 5. Only the competitive, non-competitive, and inhibition-free models are considered. Notably, the inhibition-free model describes the initial rates reasonably well at low substrate concentrations but fails at higher concentrations.

Both the competitive and non-competitive inhibition models show very similar behavior and deviate only above substrate concentrations of approximately 500 mM. When calculated with a product concentration of 0 mM, both inhibition models systematically overestimate the measured initial rates, which correspond to the first 10 min of the reaction. At 50 mM product concentration, the simulated reaction rate is already slightly reduced due to product inhibition, and this effect is captured by both models. At this concentration, both models provide a reasonable description of the data, with the competitive inhibition model performing particularly well.

Because initial rate measurements were obtained from samples taken within the first 10 min, product accumulation during this period already reached concentrations at which mild product inhibition could influence the observed rates. This effect becomes especially relevant at high initial substrate concentrations (>1000 mM), where product concentrations of 50 mM can be reached within 10 min. Thus, in retrospect, slight product inhibition was already implicitly included in the initial rate measurements.

This further emphasizes the value of progress-curve analysis when the extent of product inhibition is unknown. In the following section, this approach is applied to further evaluate the system. The resulting kinetic parameters are compared with those obtained for a biphasic system without particles under identical conditions, as well as under reduced mixing intensity.

3.3. Comparison with biphasic system

The progress curve analysis for the biphasic system was performed similarly to the Pickering emulsion, but only competitive and non-competitive inhibition models were considered. The fit for non-competitive product inhibition is shown in Fig. 6 and the fit for competitive inhibition can be found in Figure S12.

The parameter estimates and model selection criteria for the biphasic system (Table 3) do not reveal a significant difference between the competitive and non-competitive inhibition models. However, the reduced chi-squared values (χ^2_v) suggest that the models fit the data too closely relative to the assumed experimental uncertainty. This likely indicates that the measurement errors were overestimated, resulting in overly broad confidence intervals. Nonetheless, in comparison to the Pickering emulsion, two observations can be made. First, similar to the Pickering emulsion, both models yield comparable values of V_{max} and K_M, with no statistically significant differences based on their respective confidence intervals. Second, both models produce higher product inhibition constants K_P than those obtained for the Pickering emulsions.

A higher K_P implies that product inhibition becomes relevant only at higher product concentrations. Thus, the presence of particles appears to lower the apparent product concentration required to effectively inhibit the enzyme. It is known that *p*-NP adsorbs onto neutral and negatively charged silica surfaces [59]. Given its pK_a of approximately 7.2 [59], a substantial fraction of p-NP is present in its deprotonated form under the conditions studied. Since positively charged particles are used here, adsorption of the negatively charged nitrophenolate species can be postulated. If this adsorption onto the

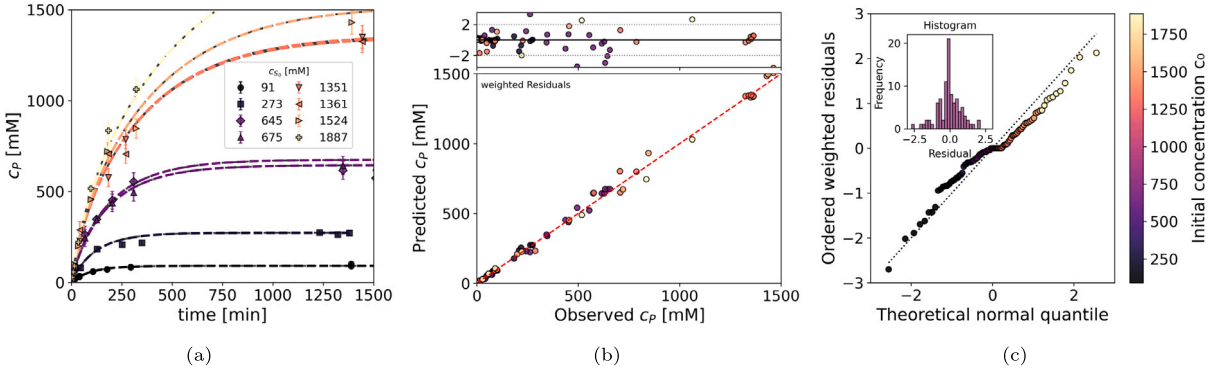

Fig. 6. (a) Non-competitive product inhibition for a biphasic system without the addition of particles. Enzyme concentration was 1g/L with respect to the aqueous phase. (b) Observed experimental data points vs. predicted product concentration, along with weighted residuals. (c) The Q-Q plot of the weighted residuals. Deviation from the identity line depicts deviation from a normal distribution.

Table 3
Parameter estimates with the respective confidence intervals for different product inhibition alongside model evaluation criteria for biphasic system stirred at 300 min^{-1}.

Inhibition type	u	CI[a] ±%	K_M	CI ±%	K_P	CI ±%	AIC	BIC	R^2_{adj}	χ^2_v	R^2_{pred}
comp.	44.0	11.5	839.9	20.5	209.9	18.9	629	637	0.997	0.625	0.996
noncomp.	54.4	13.1	1166.0	19.2	438.4	18.3	632	640	0.997	0.697	0.996

u in μmol min^{-1} mg^{-1}; K_M and K_P in mM.
[a] CI denotes the 95% confidence interval.

particles is reversible and does not completely immobilize the product, the diffusion of product into the bulk phase is potentially reduced. This, in turn, increases the product concentration at the interface, where the enzyme resides. Consequently, the corresponding bulk concentration is lower, and inhibition is observed at lower bulk concentrations.

To further validate this hypothesis, interfacial tension measurements of the octanol/water system in the presence of both *p*-NP and nanoparticles were performed (Figure S8). Experimental details are provided in the Supplementary Material. The adsorption of the positively charged nanoparticles at the interface and their corresponding reduction of the interfacial tension have been discussed previously [32]. Upon the progressive addition of *p*-NP, the effect of the nanoparticles on the interfacial tension became increasingly suppressed. Since *p*-NP itself did not exhibit any measurable interfacial activity, these results suggest that *p*-NP adsorbs onto the nanoparticle surface, thereby reducing the particles' ability to spontaneously adsorb at the interface. However, further investigations are required to fully substantiate this observation.

3.4. Comparison with biphasic system under reduced stirring

Since using a Pickering emulsion does not increase reaction rate but seems to even slightly enhance product inhibition, the advantage of using Pickering emulsions for biocatalysis becomes questionable. The main reported benefit of biocatalytic Pickering emulsions over conventional biphasic systems is the enlarged interfacial area, which often leads to increased reaction rates [6–10]. However, this relationship is not straightforward, as part of the interfacial area is occupied by the stabilizing particles and mass transfer may become limited under certain conditions [60]. Figure S9 presents the initial reaction rates of Pickering emulsions at varying particle concentrations alongside the corresponding Sauter mean diameters. While increasing the particle concentration from 0.1 wt% to 0.5 wt% approximately doubles the interfacial area, the reaction rate increases by only 24% at a substrate concentration of 5.5 mM. At 50 mM substrate concentration, the effect on the reaction rate is negligible, indicating that the increase in interfacial area does not directly translate into a proportional increase in catalytic activity. Reported catalytic enhancements range from a modest 1.2-fold increase [61] up to a 300-fold improvement compared to biphasic systems [6].

However, such performance gains are highly system-dependent and are strongly influenced by the enzyme type, its availability at the interface, the solvent environment, and the applied energy input through stirring, both for Pickering emulsions and conventional biphasic systems. Moreover, in many studies a direct comparison to an appropriate biphasic reference system is not provided.

Specifically for this system, the relatively low interfacial tension of the octanol/water interface is further reduced by enzyme adsorption to approximately 3.2 mN/m [32], thereby facilitating droplet breakup. In addition, the interfacial elasticity of the enzyme-laden interface suppresses droplet coalescence [62]. Together, these effects promote efficient stabilization and energy storage in the form of interfacial area. For this reason, the highest measured specific activity of 21.67 μmol/min/mg for the biphasic system is in the same order of magnitude as biocatalytic Pickering emulsions in other studies [7,8,19].

Furthermore, it was found that the accumulation of product destabilizes the emulsions at high product concentration. For experiments performed with substrate concentrations up to 630 mM, the interface remained largely stable and droplets could still be observed. At 740 mM, clear phase separation at the end of the reaction occured. This effect was even more pronounced when p-NP was added directly and the emulsion was unstable at a concentration of 540 mM. The presence of butyric acid did not destabilize the interface on its own and even prevented destabilization by p-NP at slightly higher concentrations. Due to the acidity of the butyric acid, p-NP should be shifted to the neutrally charged species. This further supports the proposed adsorption of the negatively charged nitrophenolate at the positively charged particles.

To ensure that these datapoints did not skew the resulting parameters and conclusions for the Pickering emulsions, the fit was repeated excluding datapoints above 740 mM. The corresponding parameters are summarized in Tables S1 and S2. No significant differences from the parameters obtained using the complete dataset were observed.

In contrast to Pickering emulsions, the dynamic biphasic interface coalesces once the energy input is stopped, whereas particle-stabilized interfaces remain stable for several weeks. The interfacial area for the biphasic system is thus directly proportional to the stirring speed whereas it stays constant for a Pickering emulsion. It was previously demonstrated that the advantage of Pickering emulsions becomes considerably more pronounced at reduced stirring speeds or even under

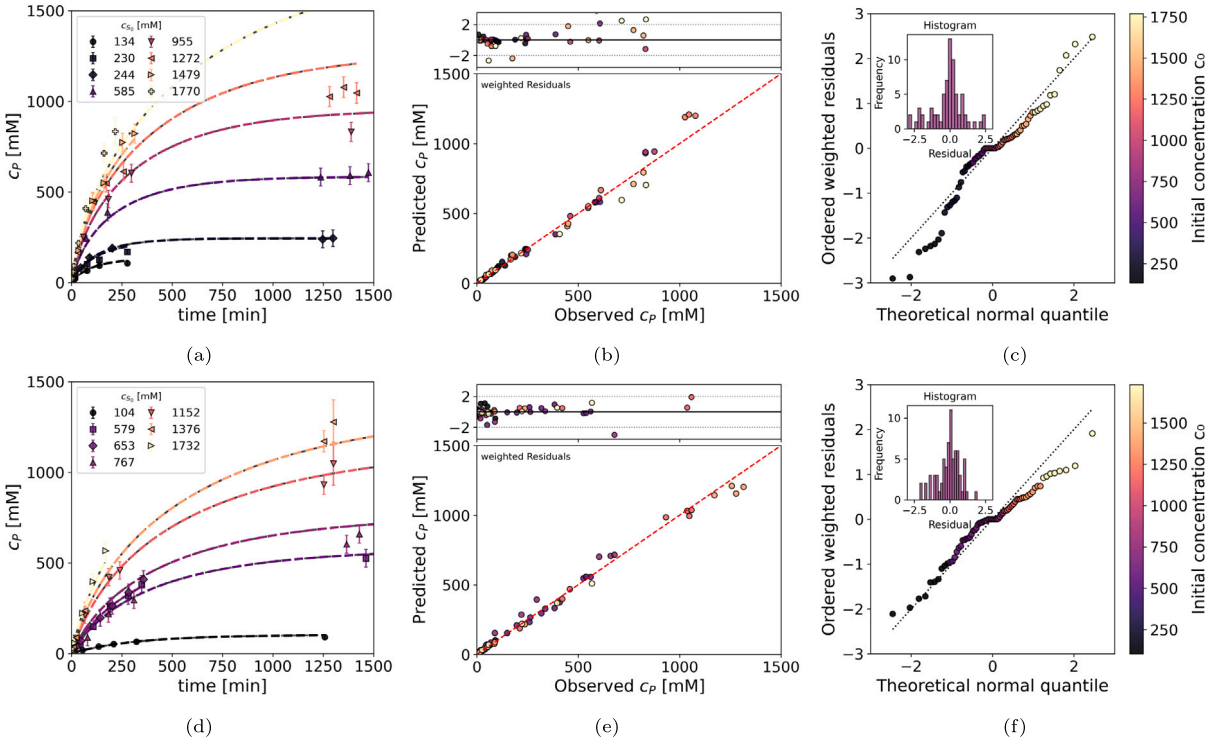

Fig. 7. Progress curve analysis in a Pickering emulsion (a–c) and biphasic system (d–f) stirred at 100 min^{-1}. Enzyme concentration was 1 g/L. Non-competitive product inhibition was fitted.

static conditions. While no activity enhancement was observed at high stirring speeds, the Pickering emulsion without stirring exhibited a 22.5-fold higher activity than the biphasic system [19].

In order to show the effect of reduced energy input on the obtained kinetics, stirring speed was set to 100 min^{-1} for both the biphasic system and the Pickering emulsion. A noncompetitive product inhibition fit is considered for comparison and is shown in Fig. 7. The respective parameters are summarized in Table 4.

The estimated parameters for the Pickering emulsion remained consistent when the stirring speed was reduced to 100 min^{-1}. In contrast, the biphasic system exhibited a significant reduction in reaction rate. Microscopy images acquired immediately after stirring revealed droplet diameters of approximately 177 µm and 426 µm at stirring rates of 300 min^{-1} and 100 min^{-1}, respectively (see Figure S10). The product concentrations shown in Fig. 7 indicate that complete conversion has not yet been achieved and the reaction is still taking place. However, this is strongly governed by mass transfer limitations. This becomes particularly evident when examining the fitted parameters. While a numerical solution can be obtained that provides a reasonable fit to the experimental data, the parameters are practically non-identifiable, as their confidence intervals are larger than the estimated parameter values. This is most evident in the unrealistically high K_M value, which, from a theoretical perspective, reflects the apparent decrease in substrate affinity caused by mass-transfer limitations.

Additionally, the initial rates were extracted from the progress curves and compared in Fig. 8. For the biphasic system under reduced stirring, this provides a more realistic comparison than the kinetic parameters obtained above. The increased fluctuations indicate lower accuracy when mass transfer limitations are induced. Nevertheless, the reaction rate follows an approximately linear trend over the investigated substrate range, which again leads to arbitrary parameters when fitting the Michaelis–Menten equation. This further indicates that the reaction rate is governed by mass transfer rather than intrinsic kinetics, as it becomes directly proportional to the substrate concentration in the oil phase. The parameters obtained from the initial rate fit at higher stirring (K_M = 1331 mM; u = 43.5 µmol/min/mg) are similar to the values in the Pickering emulsion in Table 1.

Table 4
Parameter estimates with the respective confidence intervals for different product inhibition alongside model evaluation criteria for biphasic system stirred at 300 min^{-1}.

System	min^{-1}	u	CI[a] ±%	K_M	CI ±%	K_P	CI ±%
PE	300	60.7	20.6	1490	28.3	236.1	15.2
Biphasic	300	54.4	13.1	1166	19.2	438.4	18.3
PE	100	64.6	20.4	1366	26.1	242.0	21.7
Biphasic[b]	100	41.6	99.8	12 442	105.1	584.0	30.3

u in µmol min^{-1} mg^{-1}; K_M and K_P in mM.
[a] CI denotes the 95% confidence interval.
[b] Parameters are practically non-identifiable.

3.5. Perspectives and limitations

From a mathematical perspective, the application of the closed-form integrated Michaelis–Menten equation represents the exact solution for a batch reaction and enables straightforward determination of kinetic parameters from progress curves [63]. Unfortunately, its applicability is currently restricted to irreversible uni–uni reaction systems. Once the reaction system becomes more complex (e.g., reactions involving multiple substrates and/or products and equlibria), a closed-form expression of the integrated equation is generally no longer available [38,64]. According to Duggleby, using the closed-form expression of complex systems is unlikely to yield reliable results [64].

When advancing to more complex reactions, e.g. esterifications, transesterifications or enzyme cascades, numerical integration of ordinary differential equation systems is typically preferred for parameter estimation and progress-curve analysis. As demonstrated for the non-competitive and uncompetitive inhibition models, this approach

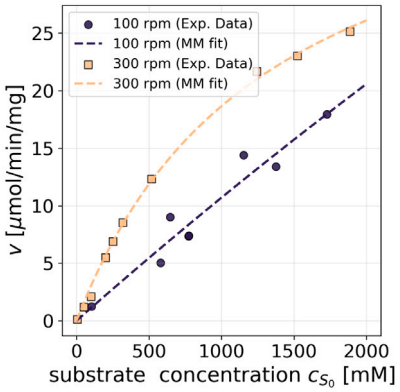

Fig. 8. Initial rates for the biphasic system for different stirring rates with respective Michaelis–Menten fit.

remains viable. However, it introduces additional mathematical challenges, including the dependence of the optimization procedure on suitable initial parameter estimates to ensure convergence [65,66].

For an irreversible two-substrate mechanism, between three and seven kinetic parameters may be required, depending on the inhibition model employed [67]. In enzyme cascades, the number of parameters increases even further [68]. Consequently, it is essential to consider multiple model evaluation criteria to obtain reliable parameter estimates and avoid overfitting. When applying such approaches to Pickering emulsions, it is important to ensure that physicochemical properties, such as droplet size and emulsion stability, remain unchanged throughout the reaction. Water formation or other compositional changes may alter these properties, thereby restricting the applicability of the kinetic model or distorting the resulting parameter estimates. The observed influence of the particles on the inhibition constant further suggests that particle concentration itself may need to be incorporated into macrokinetic models. Future studies are therefore required to assess the applicability and limitations of kinetic modeling approaches for more complex reaction systems in Pickering emulsions.

4. Conclusions

Previous studies on enzymatic reactions in multiphase systems, particularly Pickering emulsions, have lacked comprehensive descriptions of the reaction kinetics. This study therefore presented a comprehensive framework for reaction kinetics in biocatalytic W/O Pickering emulsions for a hydrolysis reaction. First, a conventional Michealis-Menten model was fitted with initial reaction rates for a single-phase system as well as a Pickering emulsion. When transitioning from the aqueous system to the Pickering emulsion, the maximum reaction velocity v_{max} increased by approximately threefold due to improved substrate solubility inside the organic solvent, while the Michaelis–Menten constant increased by three orders of magnitude. This apparent K_M likely incorporates substrate and product mass transfer through the interface.

By analyzing the full reaction progress, the kinetic parameters obtained from the initial rate analysis were able to predict the product concentration up to 250 mM reasonably well but failed at higher concentrations, indicating product inhibition. Using the integrated rate equation, the parameters could be obtained by directly fitting the full progress curve. This approach significantly reduced the experimental effort required to account for product inhibition and highlights its advantage over initial rate analysis.

Competitive, non-competitive, and uncompetitive inhibition models were compared. For the progress-curve analysis, both the non-competitive and competitive inhibition models described the data equally well, whereas the parameters of the uncompetitive model were not identifiable. The availability of a closed-form solution for the competitive inhibition model substantially reduced computational time, which is a major advantage for implementation in dynamic system models such as moving-horizon estimation.

This method was further applied to compare kinetic parameters with those of a biphasic system without particles. At high stirring speeds, the biphasic system showed comparable reaction rates and kinetic parameters, although the inhibition constant K_P increased. The stronger apparent product inhibition was attributed to adsorption of the product onto the particles. When the energy input through stirring was reduced, the Pickering emulsion retained its enzymatic activity and kinetic parameters, whereas the biphasic system exhibited a reduced reaction rate with kinetics dominated by mass-transfer limitations.

This work provides quantified kinetic parameters within a Pickering emulsion - data that has been largely lacking in literature but is crucial for industrial scaling. The advantages of progress-curve analysis for enzymatic reactions in the presence of product inhibition was elucidated. With the obtained parameters being specific for the respective reaction, enzyme and system, this work may further serve as a framework to quantify reaction kinetics within biphasic media.

Nomenclature

Symbol	Description	Unit
AIC	Akaike information criterion	–
BIC	Bayesian information criterion	–
c_E	Enzyme concentration	g/L
c_S	Substrate concentration	mM
c_P	Product concentration	mM
c_{S_0}	Initial substrate concentration	mM
CI	Confidence Interval	–
J	Jacobian matrix	–
k	Number of parameters	–
n	Number of datapoints	–
r	Reaction rate	µmol/L/min
u	Specific maximum reaction rate	µmol/min/mg
$v_{\max}$	Maximum reaction rate	µmol/L/min
v	Specific reaction rate	µmol/min/mg
V	Volume	L
W	Lambert-W function	–
K_M	Michaelis–Menten constant	mM
K_P	Product inhibition constant	mM
ϕ	Aqueous phase fraction	–
P	Partition coefficient	–
k_{cat}	Turnover number	s^{-1}
χ^2_v	Reduced chi-squared statistic	–

CRediT authorship contribution statement

Maximilian Seiler: Writing – original draft, Visualization, Validation, Software, Methodology, Investigation, Formal analysis, Data curation, Conceptualization. **Thomas Waluga:** Writing – review & editing, Methodology, Conceptualization. **Anja Drews:** Writing – review & editing, Supervision, Resources, Project administration.

Declaration of competing interest

The authors declare that they have no known competing financial interests or personal relationships that could have appeared to influence the work reported in this paper.

Appendix A. Supplementary data

Supplementary material related to this article can be found online at https://doi.org/10.1016/j.cej.2026.179611.

Data availability

Research Link Provided

Experimental Data and code (Original data) (github)

References

[1] W. Ramsden, Separation of solids in the surface-layers of solutions and 'suspensions' (observations on surface-membranes, bubbles, emulsions, and mechanical coagulation).—Preliminary account, Proc. R. Soc. Lond. (1904) 156–164.

[2] S.U. Pickering, CXCVI.—Emulsions, J. Chem. Soc. Trans. 91 (1907) 2001–2021, http://dx.doi.org/10.1039/CT9079102001, URL https://pubs.rsc.org/en/content/articlelanding/1907/ct/ct9079102001.

[3] B.P. Binks, Particles as surfactants—similarities and differences, Curr. Opin. Colloid Interface Sci. 7 (1) (2002) 21–41, http://dx.doi.org/10.1016/S1359-0294(02)00008-0, URL https://www.sciencedirect.com/science/article/pii/S1359029402000080.

[4] Y. Chevalier, M.-A. Bolzinger, Emulsions stabilized with solid nanoparticles: Pickering emulsions, Colloids Surf. A 439 (2013) 23–34, http://dx.doi.org/10.1016/j.colsurfa.2013.02.054, URL https://www.sciencedirect.com/science/article/pii/S092775751300157X.

[5] E. Guzmán, Pickering emulsions in catalytic processes, ChemCatChem 16 (20) (2024) e202400856, http://dx.doi.org/10.1002/cctc.202400856, URL https://onlinelibrary.wiley.com/doi/abs/10.1002/cctc.202400856.

[6] C. Wu, S. Bai, M.B. Ansorge-Schumacher, D. Wang, Nanoparticle cages for enzyme catalysis in organic media, Adv. Mater. 23 (47) (2011) 5694–5699, http://dx.doi.org/10.1002/adma.201102693, URL https://onlinelibrary.wiley.com/doi/abs/10.1002/adma.201102693.

[7] L. Liu, L. Jiang, X. Xie, S. Yang, Amphiphilic carbonaceous microsphere-stabilized oil-in-water Pickering emulsions and their applications in enzyme catalysis, ChemPlusChem 81 (7) (2016) 629–636, http://dx.doi.org/10.1002/cplu.201600127, URL https://onlinelibrary.wiley.com/doi/abs/10.1002/cplu.201600127.

[8] L. Peng, A. Feng, S. Liu, M. Huo, T. Fang, K. Wang, Y. Wei, X. Wang, J. Yuan, Electrochemical stimulated Pickering emulsion for recycling of enzyme in biocatalysis, ACS Appl. Mater. Interfaces 8 (43) (2016) 29203–29207, http://dx.doi.org/10.1021/acsami.6b09920.

[9] Q. Tian, J. Zhang, J. Yan, S. Zhang, Z. Yu, Enzyme anchoring amphiphilic polymer nanoparticles for enhanced Pickering interfacial biocatalysis, ACS Appl. Polym. Mater. 5 (3) (2023) 1747–1755, http://dx.doi.org/10.1021/acsapm.2c01868.

[10] Z. Wang, M.C.M. van Oers, F.P.J.T. Rutjes, J.C.M. van Hest, Polymersome colloidosomes for enzyme catalysis in a biphasic system, Angew. Chem. - Int. Ed. 51 (43) (2012) 10746–10750, http://dx.doi.org/10.1002/anie.201206555, URL https://onlinelibrary.wiley.com/doi/abs/10.1002/anie.201206555.

[11] J. Tang, B. Zhang, M. Zhang, H. Yang, Interfacial effects of catalysis in Pickering emulsions, J. Phys. Chem. Lett. 15 (35) (2024) 8973–8983, http://dx.doi.org/10.1021/acs.jpclett.4c01781.

[12] C. Zhang, R. Cui, L. Qi, M. Zong, C. Zhang, Y. Cao, W. Lou, Agar-based Pickering emulsion: A platform for enzymatic and chemoenzymatic synthesis, Chem. Eng. J. 522 (2025) 167562, http://dx.doi.org/10.1016/j.cej.2025.167562, URL https://www.sciencedirect.com/science/article/pii/S1385894725084013.

[13] A. Heyse, C. Plikat, M. Ansorge-Schumacher, A. Drews, Continuous two-phase biocatalysis using water-in-oil Pickering emulsions in a membrane reactor: Evaluation of different nanoparticles, Catal. Today 331 (2019) 60–67, http://dx.doi.org/10.1016/j.cattod.2017.11.032, URL https://www.sciencedirect.com/science/article/pii/S0920586117308118.

[14] Y. Jiang, X. Liu, Y. Chen, L. Zhou, Y. He, L. Ma, J. Gao, Pickering emulsion stabilized by lipase-containing periodic mesoporous organosilica particles: A robust biocatalyst system for biodiesel production, Bioresour. Technol. 153 (2014) 278–283, http://dx.doi.org/10.1016/j.biortech.2013.12.001, URL https://www.sciencedirect.com/science/article/pii/S096085241301818X.

[15] X. Liu, Y. Mao, S. Yu, H. Zhang, K. Hu, L. Zhu, J. Ji, J. Wang, An efficient and recyclable Pickering magnetic interface biocatalyst: application in biodiesel production, Green Chem. 23 (2) (2021) 966–972, http://dx.doi.org/10.1039/D0GC03527K, URL https://pubs.rsc.org/en/content/articlelanding/2021/gc/d0gc03527k.

[16] L. Adomi, A. Drews, Impact of Pickering emulsions composition on lipase catalyzed peroxyacetic acid synthesis, Chem. Ing. Tech. 96 (4) (2024) 535–544, http://dx.doi.org/10.1002/cite.202400005, URL https://onlinelibrary.wiley.com/doi/abs/10.1002/cite.202400005.

[17] K. Li, H. Zou, R. Ettelaie, J. Zhang, H. Yang, Spatial localization of two enzymes at Pickering emulsion droplet interfaces for cascade reactions, Angew. Chem. - Int. Ed. 62 (15) (2023) e202300794, http://dx.doi.org/10.1002/anie.202300794, URL https://onlinelibrary.wiley.com/doi/abs/10.1002/anie.202300794.

[18] M. Zhang, M. Wang, Y. Mi, T. Li, D. Hou, H. Li, X. Tong, T. Zhang, H. Yi, H. Yang, Enhanced enzyme stability at the interphase of water-oil for continuous-flow olefin epoxidation, Nat. Commun. 16 (1) (2025) 8087, http://dx.doi.org/10.1038/s41467-025-63476-1, URL https://www.nature.com/articles/s41467-025-63476-1.

[19] L. Wei, M. Zhang, X. Zhang, H. Xin, H. Yang, Pickering emulsion as an efficient platform for enzymatic reactions without stirring, ACS Sustain. Chem. Eng. 4 (12) (2016) 6838–6843, http://dx.doi.org/10.1021/acssuschemeng.6b01776.

[20] S. Yu, D. Zhang, J. Jiang, Z. Cui, W. Xia, B.P. Binks, H. Yang, Biphasic biocatalysis using a CO2-switchable Pickering emulsion, Green Chem. 21 (15) (2019) 4062–4068, http://dx.doi.org/10.1039/C8GC03879A, URL https://pubs.rsc.org/en/content/articlelanding/2019/gc/c8gc03879a.

[21] R. Röllig, C. Plikat, M.B. Ansorge-Schumacher, Efficient and selective carboligation with whole-cell biocatalysts in Pickering emulsion, Angew. Chem. - Int. Ed. 58 (37) (2019) 12960–12963, http://dx.doi.org/10.1002/anie.201907209, URL https://onlinelibrary.wiley.com/doi/abs/10.1002/anie.201907209.

[22] H. Zhong, R. Liu, H. Liu, Y. Zhang, Y. Liu, Y. Zhang, M. Zheng, Enhanced stability and catalytic performance of pH-responsive Pickering interface biocatalysis via electrostatically mediated immobilized enzymes, ACS Sustain. Chem. Eng. (2025) http://dx.doi.org/10.1021/acssuschemeng.5c00537.

[23] C. Wu, M. Kraume, M.B. Ansorge-Schumacher, Optimized biocatalytically active static emulsions for organic synthesis in nonaqueous media, ChemCatChem 3 (8) (2011) 1314–1319, http://dx.doi.org/10.1002/cctc.201100085, URL https://onlinelibrary.wiley.com/doi/abs/10.1002/cctc.201100085.

[24] K.A. Johnson, R.S. Goody, The original michaelis constant: Translation of the 1913 Michaelis–Menten paper, Biochemistry 50 (39) (2011) 8264–8269, http://dx.doi.org/10.1021/bi201284u.

[25] R.A. Deems, Interfacial enzyme kinetics at the phospholipid/ water interface: Practical considerations, Anal. Biochem. 287 (1) (2000) 1–16, http://dx.doi.org/10.1006/abio.2000.4766, URL https://www.sciencedirect.com/science/article/pii/S0003269700947663.

[26] O.A. Gutiérrez, M. Chavez, E. Lissi, A theoretical approach to some analytical properties of heterogeneous enzymatic assays, Anal. Chem. 76 (9) (2004) 2664–2668, http://dx.doi.org/10.1021/ac049885d.

[27] O. Kartal, O. Ebenhoeh, A generic rate law for surface-active enzymes, FEBS Lett. 587 (17) (2013) 2882–2890, http://dx.doi.org/10.1016/j.febslet.2013.07.026, URL https://www.sciencedirect.com/science/article/pii/S0014579313005553.

[28] J. Kari, J.P. Olsen, K. Jensen, S.F. Badino, K.B.R.M. Krogh, K. Borch, P. Westh, Sabatier principle for interfacial (heterogeneous) enzyme catalysis, ACS Catal. 8 (12) (2018) 11966–11972, http://dx.doi.org/10.1021/acscatal.8b03547.

[29] J. Kari, G.A. Molina, K.S. Schaller, C. Schiano-di Cola, S.J. Christensen, S.F. Badino, T.H. Sørensen, N.S. Røjel, M.B. Keller, N.R. Sørensen, B. Kolaczkowski, J.P. Olsen, K.B.R.M. Krogh, K. Jensen, A.M. Cavaleiro, G.H.J. Peters, N. Spodsberg, K. Borch, P. Westh, Physical constraints and functional plasticity of cellulases, Nat. Commun. 12 (1) (2021) 3847, http://dx.doi.org/10.1038/s41467-021-24075-y, URL https://www.nature.com/articles/s41467-021-24075-y.

[30] H. Ooka, Y. Chiba, R. Nakamura, Thermodynamic principle to enhance enzymatic activity using the substrate affinity, Nat. Commun. 14 (1) (2023) 4860, http://dx.doi.org/10.1038/s41467-023-40471-y, URL https://www.nature.com/articles/s41467-023-40471-y.

[31] S. Rusli, J. Grabowski, A. Drews, M. Kraume, A multi-scale approach to modeling the interfacial reaction kinetics of lipases with emphasis on enzyme adsorption at water-oil interfaces, Processes 8 (9) (2020) 1082, http://dx.doi.org/10.3390/pr8091082, URL https://www.mdpi.com/2227-9717/8/9/1082.

[32] M. Seiler, M. Loidolt-Krüger, R. von Klitzing, A. Drews, Effect of pH and particle charge on the interfacial properties of biocatalytic Pickering emulsions-where are the enzymes located? Langmuir 41 (37) (2025) 25264–25276, http://dx.doi.org/10.1021/acs.langmuir.5c02459.

[33] J.Y. Vang, C. Breceda, C. Her, V.V. Krishnan, Enzyme kinetics by real-time quantitative NMR (qNMR) spectroscopy with progress curve analysis, Anal. Biochem. 658 (2022) 114919, http://dx.doi.org/10.1016/j.ab.2022.114919, URL https://www.sciencedirect.com/science/article/pii/S0003269722003797.

[34] J.-M. Frère, O. Verlaine, A. Matagne, The measurement of true initial rates is not always absolutely necessary to estimate enzyme kinetic parameters, Sci. Rep. 13 (1) (2023) 15053, http://dx.doi.org/10.1038/s41598-023-41805-y, URL https://www.nature.com/articles/s41598-023-41805-y.

[35] J. Pleiss, Modeling enzyme kinetics: Current challenges and future perspectives for biocatalysis, Biochemistry 63 (20) (2024) 2533–2541, http://dx.doi.org/10.1021/acs.biochem.4c00501.

[36] K.A. Johnson, New standards for collecting and fitting steady state kinetic data, Beilstein J. Org. Chem. 15 (1) (2019) 16–29, http://dx.doi.org/10.3762/bjoc.15.2, URL https://www.beilstein-journals.org/bjoc/articles/15/2.

[37] S.M. Hanson, S. Schnell, Reactant stationary approximation in enzyme kinetics, J. Phys. Chem. A 112 (37) (2008) 8654–8658, http://dx.doi.org/10.1021/jp8026226.

[38] T. Waluga, F. von Ziegner, M. Skiborowski, Analytical and numerical approaches to the analysis of progress curves: A methodological comparison, Process. Biochem. 151 (2025) 1–13, http://dx.doi.org/10.1016/j.procbio.2025.01.029, URL https://www.sciencedirect.com/science/article/pii/S1359511325000376.

[39] S.L. Beal, On the solution to the Michaelis–Menten equation, J. Pharmacokinet. Biopharm. 10 (1) (1982) 109–119, http://dx.doi.org/10.1007/BF01059186.
[40] M. Goličnik, The integrated Michaelis–Menten rate equation: déjà vu or vu jàdé? J. Enzym. Inhib. Med. Chem. 28 (4) (2013) 879–893, http://dx.doi.org/10.3109/14756366.2012.688039.
[41] S. Schnell, C. Mendoza, Closed form solution for time-dependent enzyme kinetics, J. Theoret. Biol. 187 (2) (1997) 207–212, http://dx.doi.org/10.1006/jtbi.1997.0425, URL https://www.sciencedirect.com/science/article/pii/S0022519397904252.
[42] S. Schnell, C. Mendoza, Time-dependent closed form solutions for fully competitive enzyme reactions, Bull. Math. Biol. 62 (2) (2000) 321–336, http://dx.doi.org/10.1006/bulm.1999.0156.
[43] G. Deogratias, M. Madirisha, F. Jacob, Explicit solutions for real-time reversible inhibition kinetics using lambert W function: Towards progress curve analysis, Tanzan. J. Sci. 48 (4) (2022) 886–896, http://dx.doi.org/10.4314/tjs.v48i4.15, URL https://www.ajol.info/index.php/tjs/article/view/238949.
[44] M. Seiler, S. Stock, A. Drews, pH-dependent electrostatic interactions between enzymes and nanoparticles in Pickering emulsions - influence on activity and droplet size, J. Biotechnol. (2024) 28–36, http://dx.doi.org/10.1016/j.jbiotec.2024.01.006, URL https://www.sciencedirect.com/science/article/pii/S0168165624000142.
[45] S. Stock, A. Schlander, M. Kempin, R. Geisler, D. Stehl, K. Spanheimer, N. Hondow, S. Micklethwaite, A. Weber, R. Schomäcker, A. Drews, M. Gallei, R.v. Klitzing, The quantitative impact of fluid vs. solid interfaces on the catalytic performance of Pickering emulsions, Phys. Chem. Chem. Phys. 23 (3) (2021) 2355–2367, http://dx.doi.org/10.1039/D0CP06030E, URL https://pubs.rsc.org/en/content/articlelanding/2021/cp/d0cp06030e.
[46] J. Pliego, J.C. Mateos, J. Rodriguez, F. Valero, M. Baeza, R. Femat, R. Camacho, G. Sandoval, E.J. Herrera-López, Monitoring lipase/esterase activity by stopped flow in a sequential injection analysis system using p-nitrophenyl butyrate, Sensors 15 (2) (2015) 2798–2811, http://dx.doi.org/10.3390/s150202798, URL https://www.mdpi.com/1424-8220/15/2/2798.
[47] E. Vanleeuw, S. Winderickx, K. Thevissen, B. Lagrain, M. Dusselier, B.P.A. Cammue, B.F. Sels, Substrate-specificity of candida rugosa lipase and its industrial application, ACS Sustain. Chem. Eng. 7 (19) (2019) 15828–15844, http://dx.doi.org/10.1021/acssuschemeng.9b03257.
[48] N. López, M.A. Pernas, L.M. Pastrana, A. Sánchez, F. Valero, M.L. Rúa, Reactivity of pure candida rugosa lipase isoenzymes (Lip1, Lip2, and Lip3) in aqueous and organic media. influence of the isoenzymatic profile on the lipase performance in organic media, Biotechnol. Prog. 20 (1) (2004) 65–73, http://dx.doi.org/10.1021/bp034188c, URL https://onlinelibrary.wiley.com/doi/abs/10.1021/bp034188c.
[49] Z. Chen, C. Zhao, E. Ju, H. Ji, J. Ren, B.P. Binks, X. Qu, Design of surface-active artificial enzyme particles to stabilize Pickering emulsions for high-performance biphasic biocatalysis, Adv. Mater. 28 (8) (2016) 1682–1688, http://dx.doi.org/10.1002/adma.201504557, URL https://onlinelibrary.wiley.com/doi/abs/10.1002/adma.201504557.
[50] L. Rúa, T. Díaz-Mauriño, V.M. Fernández, C. Otero, A. Ballesteros, Purification and characterization of two distinct lipases from Candida cylindracea, Biochim. Biophys. Acta 1156 (2) (1993) 181–189, http://dx.doi.org/10.1016/0304-4165(93)90134-t.
[51] M.M. Bradford, A rapid and sensitive method for the quantitation of microgram quantities of protein utilizing the principle of protein-dye binding, Anal. Biochem. 72 (1) (1976) 248–254, http://dx.doi.org/10.1016/0003-2697(76)90527-3, URL https://www.sciencedirect.com/science/article/pii/0003269776905273.
[52] Statistical inference, in: Nonlinear Regression, John Wiley & Sons, Ltd, 1989, pp. 191–269, http://dx.doi.org/10.1002/0471725315.ch5, URL https://onlinelibrary.wiley.com/doi/abs/10.1002/0471725315.ch5.
[53] G.C. Cawley, N.L.C. Talbot, On over-fitting in model selection and subsequent selection bias in performance evaluation, J. Mach. Learn. Res. 11 (70) (2010) 2079–2107, URL http://jmlr.org/papers/v11/cawley10a.html.
[54] S.-W. Tsai, G.-H. Wu, C.-L. Chiang, Kinetics of enzymatic hydrolysis of olive oil in biphasic organic-aqueous systems, Biotechnol. Bioeng. 38 (7) (1991) 761–766, http://dx.doi.org/10.1002/bit.260380710, URL https://onlinelibrary.wiley.com/doi/abs/10.1002/bit.260380710.
[55] M. Martinelle, K. Hult, Kinetics of acyl transfer reactions in organic media catalysed by *Candida antarctica* lipase B, Biochim. Biophys. Acta (BBA) - Protein Struct. Mol. Enzym. 1251 (2) (1995) 191–197, http://dx.doi.org/10.1016/0167-4838(95)00096-D, URL https://www.sciencedirect.com/science/article/pii/016748389500096D.
[56] F. Bjoerkling, J. Boutelje, S. Gatenbeck, K. Hult, T. Norin, P. Szmulik, The effect of dimethyl sulfoxide on the enantioselectivity in the pig liver esterase catalyzed hydrolysis of dialkylated propanedioic acid dimethyl esters, Bioorg. Chem. 14 (2) (1986) 176–181, http://dx.doi.org/10.1016/0045-2068(86)90028-3, URL https://www.sciencedirect.com/science/article/pii/0045206886900283.
[57] J.M. Palomo, M. Fuentes, G. Fernández-Lorente, C. Mateo, J.M. Guisan, R. Fernández-Lafuente, General trend of lipase to self-assemble giving bimolecular aggregates greatly modifies the enzyme functionality, Biomacromolecules 4 (1) (2003-02) 1–6, http://dx.doi.org/10.1021/bm025729+.
[58] S. Schnell, Validity of the Michaelis–Menten equation – steady-state or reactant stationary assumption: that is the question, FEBS J. 281 (2) (2014) 464–472, http://dx.doi.org/10.1111/febs.12564, URL https://onlinelibrary.wiley.com/doi/abs/10.1111/febs.12564.
[59] B.L. Woods, R.A. Walker, pH effects on molecular adsorption and solvation of p-nitrophenol at silica/aqueous interfaces, J. Phys. Chem. A 117 (29) (2013) 6224–6233, http://dx.doi.org/10.1021/jp400482v.
[60] M. Petzold, S. Röhl, L. Hohl, D. Stehl, M. Lehmann, R. von Klitzing, M. Kraume, Mass transfer and drop size distributions in reactive nanoparticle-stabilized multiphase systems, Chem. Ing. Tech. 89 (11) (2017) 1561–1573, http://dx.doi.org/10.1002/cite.201700060, URL https://onlinelibrary.wiley.com/doi/abs/10.1002/cite.201700060.
[61] R. Varshney, S. Kumar, K. Ghosh, D. Patra, Fabrication of dual catalytic microcapsules by mesoporous graphitic carbon nitride (mpg-C3N4) nanoparticle–enzyme conjugate stabilized emulsions, New J. Chem. 44 (7) (2020) 3097–3102, http://dx.doi.org/10.1039/C9NJ05322K, URL https://pubs.rsc.org/en/content/articlelanding/2020/nj/c9nj05322k.
[62] T.C. Botti, A. Hutin, E. Quintella, M.S. Carvalho, Effect of interfacial rheology on drop coalescence in water–oil emulsion, Soft Matter 18 (7) (2022) 1423–1434, http://dx.doi.org/10.1039/D1SM01382C, URL https://pubs.rsc.org/en/content/articlelanding/2022/sm/d1sm01382c.
[63] M. Goličnik, Closed-form solution of the reduced haldane equation for enzyme kinetics with strong substrate inhibition, Match-Commun. Math. Co 79 (2018) 607–618.
[64] R.G. Duggleby, Quantitative analysis of the time courses of enzyme-catalyzed reactions, Methods 24 (2) (2001) 168–174, http://dx.doi.org/10.1006/meth.2001.1177, URL https://www.sciencedirect.com/science/article/pii/S1046202301911776.
[65] R.G. Duggleby, Analysis of enzyme progress curves by nonlinear regression, in: Methods in Enzymology, vol. 249, Academic Press, 1995, pp. 61–90, http://dx.doi.org/10.1016/0076-6879(95)49031-0, URL https://www.sciencedirect.com/science/chapter/bookseries/abs/pii/0076687995490310.
[66] S.V. Archontoulis, F.E. Miguez, Nonlinear regression models and applications in agricultural research, Agron. J. 107 (2) (2015) 786–798, http://dx.doi.org/10.2134/agronj2012.0506, URL https://onlinelibrary.wiley.com/doi/abs/10.2134/agronj2012.0506.
[67] T. Waluga, P. Nagshi, On over-parameterisation and parameter estimation of enzyme kinetics, AppliedChem 6 (2) (2026) 25, http://dx.doi.org/10.3390/appliedchem6020025, URL https://www.mdpi.com/2673-9623/6/2/25.
[68] J. Johannsen, F. Meyer, C. Engelmann, A. Liese, G. Fieg, P. Bubenheim, T. Waluga, Multi-enzyme cascade reaction in a miniplant two-phase-system: Model validation and mathematical optimization, AIChE J. 67 (4) (2021) e17158, http://dx.doi.org/10.1002/aic.17158, URL https://onlinelibrary.wiley.com/doi/abs/10.1002/aic.17158.